ISSN: 0975-8585

Research Journal of Pharmaceutical, Biological and Chemical Sciences

Efficiency of Non-Ionic Surfactants Based On Oleic Acid as Corrosion Inhibitors for Carbon Steel Pipelines in Deep Oil Formation Water Saturated with CO_2 at 40 ºC.

Migahed MA[1], Al-Sabagh AM [1], Mishrif MR[1], Abd-El-Bary HM[2], Mohamed ZM[3], and Hussein BM*[4].

[1] Egyptian Petroleum Research Institute (EPRI), Nasr City, Cairo, Egypt.
[2] Faculty of Science, Al-Azhar University, Nasr City, Cairo, Egypt.
[3] EGPC, Palestine Street part 4, New Maadi, Cairo, Egypt.
[4] E-Gas, Company, Nasr City, Cairo, Egypt.

ABSTRACT

Preparation of nonionic surfactants from Oleic acid and their application in the field of corrosion inhibitors are the main goal of the present work. In this respect, oleic acid reacted with maleic anhydride using Diles Alder reaction to produce adduct, which esterified with ethoxthylated aniline to produce branched nonionic surfactants. The effect of ethylene oxide modification on both surface activity and corrosion inhibition efficiency on carbon steel pipelines in deep oil wells' formation water saturated with CO_2 at 40 ºC was studied by both potentiodynamic polarization techniques and electrochemical impedance spectroscopy (EIS) measurements. The corrosion inhibition efficiency of the synthesized nonionic surfactants is correlated with surface tension measurements data. The nature of protective film formed on carbon steel surface is studied by scanning electron microscopy (SEM) and energy dispersive analysis of X-rays (EDX) techniques. Polarization curves indicated that the studied inhibitors acted as mixed (cathodic /anodic) inhibitors. EIS data showed that the values of charge transfer resistance (R_t) increased by increasing the inhibitor concentration, while the values of electrochemical double layer capacitance (C_{dl}) decreased. Finally, quantum chemical calculation showed a good correlation between quantum chemical parameters for the investigated compound and their inhibition efficiencies.

Keywords: Diles Alder reaction, Carbon Steel, Corrosion in CO_2, Polarization, SEM, EIS, Surfactants, Inhibitors.

Corresponding author

ISSN: 0975-8585

INTRODUCTION

Oil wells' Formation water that naturally exists in the rocks before drilling contains a variety of dissolved organic and inorganic compounds. This water considers the most corrosive environments in oil field operations due primarily to the presence of large quantities of the corrosive carbon dioxide and hydrogen sulfide in addition to other aggressive salts such as chloride and sulfate [1-3]. The severity of corrosion depends on temperature, fluid characteristics (CO_2, partial pressure, gas / liquid ratio, formation water composition, water-to-oil ratio, and pH), flow characteristics and material characteristics. When CO_2 is present in the gas phase, any water in contact with this gas will dissolve CO_2, forming carbonic acid which is corrosive to steel [4].Steel pipelines play an important role in transporting gases and liquids throughout the world [5].Therefore, the prevention of metals used in petroleum field and industrial applications from corrosion is vital, that must be dealt with [6, 7]. Corrosion protection by organic inhibitors is mostly based on modification of the metal surface through the adsorption of inhibitor molecules and the subsequent formation of a protective blocking layer [8-11]. Surfactant corrosion inhibitors have many advantages such as high inhibition efficiency, low price, low toxicity, and easy production. Surfactants are molecules composed of a polar hydrophilic group, the ‘‘head’’, attached to a non-polar hydrophobic group, the ‘tail’’ [1, 8]. The adsorption of the surfactant molecules through their hydrophilic head changes the corrosion resistance property of the metal [6]. Generally, in aqueous solution the inhibitory action of surfactant molecules may also be due to physical (electrostatic) adsorption or chemisorptions onto the metallic surface, depending on the charge of the solid surface and the free energy change of transferring a hydrocarbon chain from water to the solid surface [8, 12 and 13]. The aim of this study is to investigate the effectiveness of some new synthesized nonionic surfactants based on Diels Alder reaction for some ethoxylated unsaturated fatty acids as corrosion inhibitors for carbon steel in oil wells’ formation water using electrochemical techniques.

Corrosion inhibition in its various forms is successfully used in many fields. In some cases the success of inhibition can be attributed to the wells being low pressure, low temperature oil wells with little water. There are two main methods for injecting inhibitor into a well stream. The first method is to inject down a dedicated treater string enabling continuous injection, and the second is to bullhead at periodic intervals down the tubing with the well shut in. The former is by far the most effective and is potentially suitable for deep, HP/HT, hostile wells.

In considering the feasibility of using carbon steel, the potential general corrosion rate by CO_2, has to be calculated. Laboratory work on CO_2 corrosion has continued to be very active throughout the last five years and has yielded interesting developments and refinements in the modelling of CO_2 corrosion. Several methods now exist for predicting the CO_2 corrosion rate of carbon and low alloy steels, and these have been brought together in one publication of the European Federation of Corrosion (EFC) [14]. CO_2 corrosion, also called sweet corrosion, involves the interactions between steel, water and CO_2. In the light of common and expensive problems occurring in the oil and gas industry, carbon dioxide corrosion has been extensively studied in the past few decades. CO_2 corrosion was also referred to as “acid corrosion” due to the major chemical reaction include CO_2 and hydration to form a weak carbonic acid (1) to (5).

$$CO_2[g] \leftrightarrow CO_2\ [aq] \quad (1)$$

$$CO_2[aq] + H_2O \leftrightarrow H_2CO_3\ [aq] \quad (2)$$

$$H_2CO_3\ [aq] \leftrightarrow H^+ + HCO_3^- \quad (3)$$

$$HCO_3\text{-} \leftrightarrow H^+ + CO_3^- \quad (4)$$

$$2H^+ + 2e^- \rightarrow H_2 \quad (5)$$

Compared to strong acids, such as hydrochloric acid (HCl) and sulfuric acid (H_2SO_4), which can completely dissociate in water, carbon acid is considered a weak acid, which dissociates only partially in water. The aqueous CO_2 corrosion of carbon steel is an electrochemical process occurring at the steel surface. The overall reaction is given by:

$$Fe + CO_2 + H_2O \leftrightarrow FeCO_3 + H_2 \quad (6)$$

When the concentration of Fe^{+2} and $(CO_3)^{-2}$ ions exceed the solubility limit , they combine to form solid iron carbonate films which is called (corrosion product film , iron carbonate $FeCO_3$ forms in CO_2

ISSN: 0975-8585

corrosion, which can remain dissolved or precipitate on the steel surface. The electrochemical reactions include anodic (oxidation) and cathodic (reduction) reactions, which have been investigated extensively in the past. The main anodic reaction is the dissolution of iron to give ferrous ions, equations (2-6).

$$Fe \leftrightarrow Fe^{+2} + 2e^{-} \quad (7)$$

The mechanism and kinetics of iron dissolution proposed **[15]** by is:

$$Fe + OH^{-} \leftrightarrow Fe(OH) + e^{-} \quad (8)$$

$$Fe(OH) \rightarrow FeOH^{+} + e^{-} \quad (9)$$

$$FeOH^{+} \rightarrow Fe^{+2} + OH^{-} \quad (10)$$

An activated complex, FeOH is formed by reaction of iron and hydroxide ion (OH^{-}). The rate determining step is dependent on the FeOH concentration [7].

EXPERIMENTAL AND TECHNIQUES

Synthesis of Novel Nonionic Surfactants

Ethoxylation of Aniline

Three ethoxylated aniline with different ethylene oxide units were prepared.**[16,17]**.The ethoxylated product is appeared as a brown viscous liquid, named as ethoxylated aniline **($E_{15}A$, $E_{25}A$ and $E_{35}A$,)**.

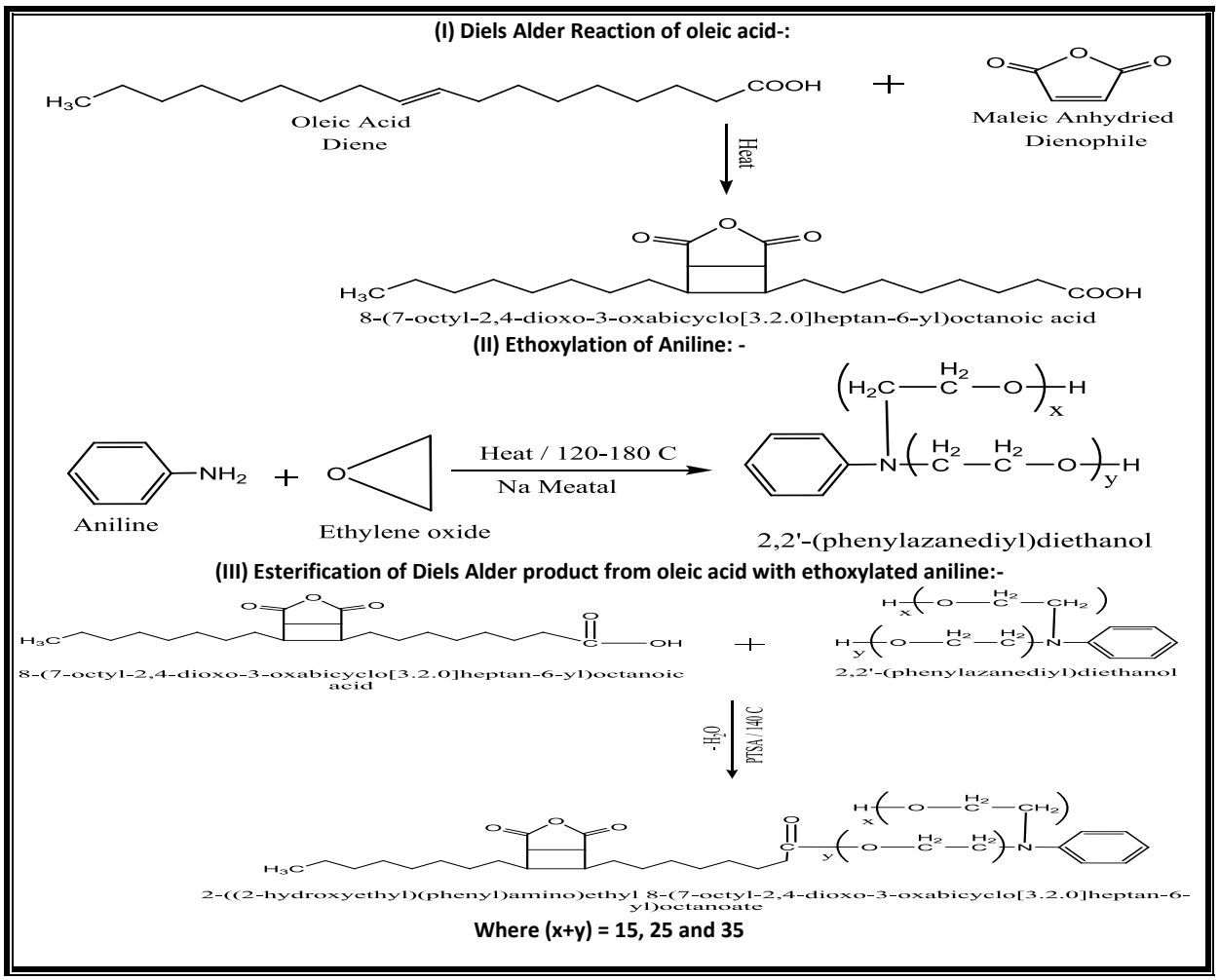

Scheme 1 of nonionic surfactants preparation

Maleic Anhydride-Oleic Acid Adduct (Diels Alder Reaction)

The produced adduct was obtained as dark brown liquid and denoted as (MOA) for maleic anhydride-Oleic acid adduct. [10]

Esterification of Maleic Anhydride – Oleic Acid Adduct

Esterified maleic anhydride – oleic acid adduct are prepared using the ethoxylated aniline ($E(_{x+y)}$ A) [18]. Inhibitor I, II and III are obtained through the reaction of maleic anhydride - oleic acid adduct with compounds ($E_{15}A$, $E_{25}A$, and $E_{35}A$) see scheme1.

Surface Tension and Surface Active Properties

Surface tension is measured for different concentrations of the synthesized nonionic surfactants dissolved in distilled water at 30 ºC. The measured values of (γ) are plotted against lnC of the surfactant concentration; the intercept of the two straight lines designates the critical micelle concentration where saturation in the surface adsorbed layer takes place. The surface active properties of the surfactant, effectiveness (π_{cmc}), maximum surface excess (Γ_{max}) and minimum area per molecule (A_{min}) were calculated and discussed [19].

Formation water

The formation water used in this study was kindly supplied from Khalda-Apache "KPC" Petroleum Company, Moghra Zone, Salam Field, Western Desert, Egypt. Most oil field water contains a variety of dissolved organic and inorganic compounds, The Chemical composition of the formation water used in this work is shown in **Table 2.**

Table 2: Chemical composition and Physical properties of deep oil well formation water used in this investigation

Test	Density g/cm^3	Turbidit NTU	PH	Salinity as NaCl (mg/l)	Conductivity@ 25°C µs/cm	Total hardness (mg/l)	Sulphate (mg/l)
Result	1.0199	745	6.69	30694	76.5	2714	920
Test	Phosphat e (mg/l)	Carbonate (mg/l)	Iron (mg/l)	Chloride (mg/l)	Bi-carbonate (mg/l)	Calcium (mg/l)	Magnesium (mg/l)
Result	340	Nil	2.2	18227	550	810	193
Test	Barium (mg/l)	Cupper (mg/l)	Zinc (mg/l)	Potassium (mg/l)	T.D.S. (mg/l)	---------	--------
Result	Nile	Nil	0.35	1450	35250	-------	-------

2.4. Chemical Composition of Carbon Steel.

The working electrodes were machined out from commercial carbon steel grade X65.The surface preparation was carried out by grinding/polishing with 1200 grit of silicon carbide paper then degreasing with iso-propanol to remove any dust and scratches so that only the corrosion examined is that which occurred in the cell, and the chemical composition is listed in **Table 1**.

Table 1: Chemical composition of carbon steel alloy

Element	C	Si	Mn	P	S	Ni	Cr	Mo	V	Cu	Al	Fe
Content (Wt %)	0.09	0.22	1.52	0.01	0.05	0.04	0.02	0.004	0.002	0.02	0.04	Rust

Characterization of the prepared Surfactants

FTIR spectra were analyzed with a Nicolet FTIR spectrophotometer using KBr in a wavenumber range of 4000–500 cm^{-1} with a resolution accuracy of 4 cm^{-1} all samples were ground and mixed with KBr and then pressed to form pellets. The surface and interfacial tension measurements between water solution and styrene was measured at 25°C by means of the pendent drop technique using drop shape analyzer model DSA-100 (Kruss, Germany). In this method the shape of a pendent drop is fitted to the theoretical drop profile according to the Laplace equation ,using surface tension as one of the adjustable parameters. The error limits of these measurements are on the order of 0.1 mN/m or less. The ADSA-100 analysis required accurate density measurements, which were measured as functions of temperature and nanogels concentration with an AP Paar DMA45 MC 1296 densitometer. Pendent drops were formed on the tip of a Teflon capillary with an outside diameter of 0.1 in. and inside diameter of 0.076 in.

Electrochemical Measurements

Electrochemical open circuit potential (OCP) is carried out in acidic media. The electrode is immersed in test solution at OCP for 30 minutes at room temperature to be sufficient to attain a stable state. The polarization curves are measured by scanning rate at 1mV s-1 in range ±0.25 V in both cathodic and anodic potentials to investigate the polarization behavior. All experiments are performed at 323 K. Potentiodynamic polarization curves are obtained by changing the electrode potential automatically from - 1.2 to - 0.4 V vs. SCE. Electrochemical impedance spectroscopy (EIS) is carried out at OCP in the frequency range of 100 kHz - 10 MHz using 10 mV peak-to-peak voltage excitation. An AC sinusoid ±10 mV is applied at the corrosion potential (E_{corr}) **[20, 21]**.

Scanning Electron Microscopy (SEM)

The scanning electron microscope (SEM) is a type of electron microscope that images the sample surface by scanning it with a high energy beam of electrons in a raster scan pattern.

Energy Dispersive Analysis of X-Rays (EDX)

EDX system attached with a JEOL JSM-5410 scanning electron microscope is used for elemental analysis or chemical characterization of the film formed on carbon steel surface.

Quantum chemical study

The molecular structures of the prepared inhibitors had been fully geometric optimize by ab initio method (3-21G** basis set) with Hyperchem 7.5, the following quantum chemical parameters calculated are the energy of the highest occupied molecular orbital (E_{HOMO}, eV), the energy of the lowest unoccupied molecular orbital (E_{LUMO}, eV), the energy gap ($\Delta E = E_{HOMO} - E_{LUMO}$, eV), the dipole moment (μ, Debye), log P (lipophilicity) and the number of transferred electrons (ΔN).

RESULTS AND DISCUSSION

The Diels-Alder reaction is one of the most important C-C bond forming organic synthesis reactions in a one-step reaction it enables the regio- and stereoselective construction of five, six and seven membered carbocycles and heterocycles [22]. There is only few examples of this cycloaddition are described for unsaturated fatty acids. The reaction is based on converting of un conjugated fatty acids, such as oleic acids, which have been converted into conjuenic acid by conjugation of the double bonds undergoes Diels-Alder reactions at high temperature with dienophiles bearing electron withdrawing groups [23]. Not reported yet are Diels-Alder cycloaddition reactions of malice anhydride as dienes and fatty acid derived dienophiles. In this respect, the present work aims to prepare nonionic surfactants from Diels-Alder reaction between modified rosin ester and fatty acid. These extensions of the Diels- Alder reaction with unsaturated fatty acids are addressed in this contribution. The Diels-Alder addition of oleic acid with malice anhydride without any solvent at 150°C under nitrogen yielded the Diels–Alder adduct after a reaction time of 2 h in an isolated yield of 78% see Scheme1. The compounds was separated from the reaction mixture by column chromatography and recrystallized from petroleum ether/diethyl ether (4:1).

ISSN: 0975-8585

Structure confirmation of the synthesized inhibitors

FTIR spectroscopy

FTIR spectrum confirmed the expected functional groups in the synthesized nonionic surfactant showed the following absorption bands. The absorption peaks centered at 1770 and 1851 cm^{-1} are the two characteristic bands which correspond to the absorption of C=O of the anhydride groups in the unreacted cyclic five-membered ring. The stretching absorption bands at 2900 and 2880 cm^{-1} are assigned to ν_s and ν_{as} of the alkyl group. The peak at 1050cm^{-1} is due to the ethereal band (C-O) $_{stretching}$. It is clear that as ethylene oxide increase, the ethereal band intensity increase. The peak at 1250 cm^{-1} shows the C-N *str*etching. the peak at 701 cm^{-1} corresponds to the out-of-plan ring bending of the phenyl group and the peaks within a range of 3100-3000 cm^{-1} were due to aromatic stretching vibrations in A_n.The band at 3435 cm^{-1} is for the terminal OH stretching group of the ethylene oxide uinte. FTIR spectrum of the synthesized inhibitor is shown in **Fig. 1**.

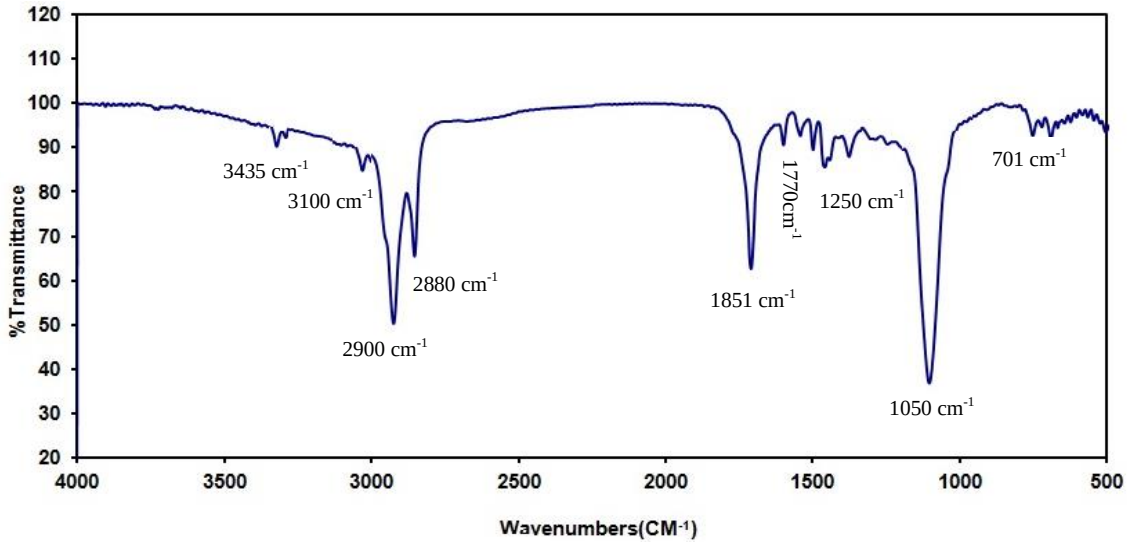

Figure 1: Finger Print for FTIR Spectra of Inhibitor III

Relationship between Critical Micelle Concentration and Degree of Ethoxylation of the Synthesized Surfactants

The CMC values of the synthesized surfactants are determined at 30 ºC from the change in the slope of the plotted data of surface tension (γ) versus the natural logarithm of the solute molar concentration. Surface tension measurements of the synthesized surfactants are shown in **Fig. 2.** The presented curves are used for estimating surface activity and confirming the purity of the studied surfactants. It is of interest to mention that all the obtained isotherms showed one phase, which is considered as an indication of the purity for the prepared surfactants. The critical micelle concentration (CMC) is the point in concentration at which it becomes thermodynamically favorable for surfactant molecules in solution to form aggregates (micelles) in order to minimize interaction of either their head groups or their tail groups with the solvent. For the under investigated surfactant, micellization is due to entropic considerations. Water molecules in close proximity to the hydrophobic group of the surfactant molecules take on a certain ordered configuration, which is entropically unfavorable. Once the surfactant concentration reaches a certain level (CMC), the water structure forces aggregation of the hydrophobic tail groups-thus forming surfactant micelles. These plots show that, the surfactant is molecularly dispersed at low concentrations leading to a reduction in surface tension. This reduction increases as the concentration of the surfactant increases. At higher concentrations, however, when a certain CMC is reached the surfactant molecules form micelle, which are in equilibrium with the free surfactant molecules. This is clear in **Fig. 3.**

ISSN: 0975-8585

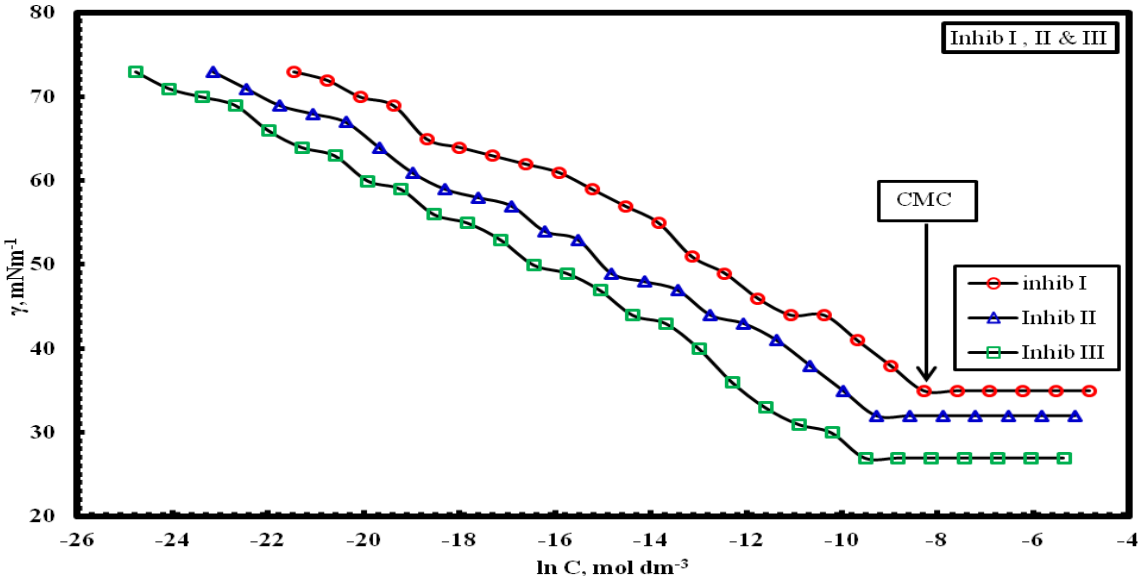

Figure 2: Surface Tension γ-ln C Adsorption Isotherm for investigated inhibitors at 30 ºC

As the concentration of surfactant molecules approaches the CMC, micelles are formed in solution, and similar aggregate structures such as bilayers and multilayers form on the surface as shown in **Fig. 3.**Further increase in surfactant concentration above the CMC results in other types of aggregates such as lamellar structures and rod-like micelles that can form in solution as well as analogous bilayers or multilayers that form at interfaces [24, 25].

Table 3: Surface Active Properties for Investigated Inhibitors at 30 ºC

Surfactants	γ cmc.mNm^{-1}	CMC x 10^{4} mol.dm^{-3}	$\Pi_{cmc.}$ mNm^{-1}	Γ_{max} x 10^{10} mol.cm^{-2}	Amin (nm molecule^{-1})
I	35	1.12	37.3	1.18	140.35
II	32	0.71	40.3	1.06	156.06
III	27	0.49	45.3	0.88	189.26

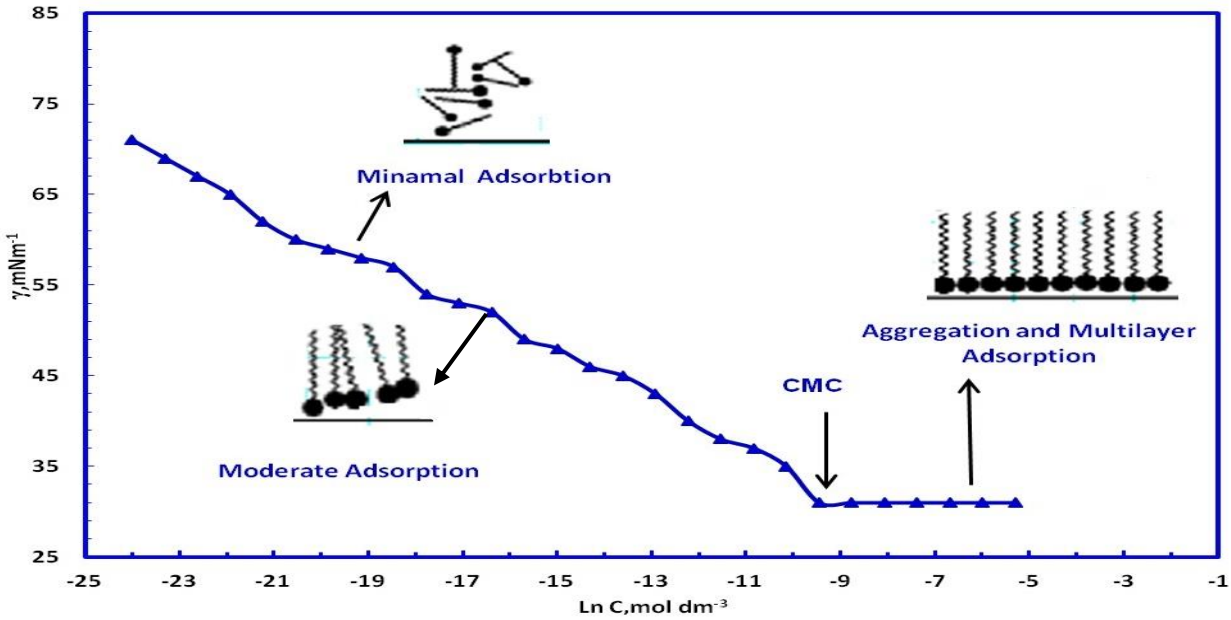

Figure 3: Change of Surface Tension γ-ln C with the concentration of the synthesized inhibitors at 30 ºC

ISSN: 0975-8585

The values of CMC and the surface tension at CMC (γ_{CMC}) are listed in **Table 3.** By careful inspection of the surface tension values, it can be concluded that, the values decrease be increasing the hydrophilic group from 15 to 35 ethylene oxide units due to the increase in the functional group which enhances the adsorption at the interface. The hydrophobic group tends to expel the surfactant molecules from the solution and enhance their departure to the interface to get away from the hydrophilic water media. The effectiveness (π_{cmc}) increased as the result of accumulating the surfactant molecules at the interface. The adsorption effectiveness of the prepared surfactants expressed by the maximum reduction of surface tension which was calculated from the equation:

$$\Delta\gamma = \gamma_{water.} - \gamma_{cmc} \qquad (11)$$

The concentration of the prepared surfactants at the solvent-air interface, Γ_{max}, and the area per molecule at the interface, A_{min} were calculated and listed in **Table 3.**The surface excess concentration of the prepared surfactants at the interface can be calculated from the surface or interfacial tension data using the following equation [26],

$$\Gamma_{max} = 1/RT \pm (-\partial\gamma/\partial \ln c)\ T \qquad (12)$$

Where $(-\partial\gamma/\partial \ln c)\ T$ is the slope of the plot of γ versus lnc at constant temperature (T), and R is the gas constant (in J mol^{-1} K^{-1}).Γ_{max} values were used for calculating the minimum area (A_{min}) at the aqueous–air interface. The area per molecule at the interface provides information about the degree of packing and the orientation of the adsorbed surfactants, when compared with the dimensions of the molecules obtained from models. From the surface excess concentration, the area per molecule at the interface is calculated using the equation:

$$A_{min} = 10^{16}/N\ \Gamma_{max} \qquad (13)$$

Where N is Avogadro's number. The area occupied at the interface is increased [26]. The maximum surface excess (Γ_{max}) is expressed as the concentration of surfactant molecules at the interface per unit area, It is clear in **Table 3** and **Fig. 3**, that the increase of hydrophilic moiety length of surfactant molecules, shift Γ_{max} to lower concentrations. The effectiveness values as well as the maximum surface excess considered as a clear description for the accumulation extent of amphiphiles molecules at the air–water interface. Decreasing the maximum surface excess values indicates the decreasing of the adsorbed molecules at the interface, hence the area available for each molecule will increase. A_{min} increased by increasing the hydrophilic moiety. Since, the molecular weight increases and the availability of the surfactant to be adsorbed on the interface per molecule will decrease. In other words, the larger the molecule, the larger the area occupied per molecule. Hence, small numbers of these surfactants will be needed to be occupied to give the best active properties.

Free Energy of Micellization.

By using the values of CMC obtained in **Table 2**, ΔG_{mic} values are listed in **Table 4.**The free energy changes of micellization and adsorption showed negative sign showing the spontaneity of the two processes at 30 ºC. The Gibbs free energies of adsorption and micellization, ΔG_{ads} and ΔG_{mic} decrease gradually by the increase in the number of ethylene oxide groups. This may be due to the increase of hydrophilic moiety of surfactant molecule which enhances the adsorption and micellization at the interface [19].It is clear that, the negativity of ΔG_{ads} and ΔG_{mic} increase with increasing the hydrophilic group. That is because the hydrophilic group in the amphiphile will be larger and the large hydrophobic group will push it to the interface to be adsorbed at large area per molecule from the interface at the sites which had greater free energy to be calmed down and be in a stable state. In other words, the increase of hydrophilic moiety of surfactant molecule enhances the adsorption and micellization at the interface.

Table 4: Thermodynamic Properties for Investigated Inhibitors at 30 ºC

Surfactants	$\Delta G_{mic.}$ (KJ mol^{-1})	$\Delta G_{ads.}$ (KJ mol^{-1})	$\Delta G_{mic.} - \Delta G_{ads}$ (KJ mol^{-1})
I	-22.92	-26.08	3.15
II	-24.06	-27.85	3.79
III	-24.99	-30.15	5.16

Moreover, ΔG_{ads} has an obvious increase in negativity than ΔG_{mic}. That showed the higher tendency of these amphiphiles towards adsorption rather than micellization then the adsorption will be accompanied with

micellization at last. The tendency towards adsorption is referred to the interaction between the aqueous phases and the hydrophobic chains which pump the amphiphile molecules to the interface [19].

Potentiodynamic Polarization Measurements

Cathodic and anodic polarization curves for carbon steel in oil wells' formation water saturated with CO_2 in the absence and presence of various concentrations of the nonionic surfactants are show in **Fig. 5.** The inhibition efficiency (IE %) was calculated using the equation 14: **[27-32]**.

$$IE\ \% = 1 - \left[\frac{I_{corr}}{I^{\circ}_{corr}}\right] \qquad (14)$$

Where I°_{corr} and I_{corr} are the corrosion current density values without and with inhibitor, respectively. The electrochemical parameters, corrosion current density (I_{corr}), corrosion potential (E_{corr}**),** anodic Tafel slope (β_a) and cathodic Tafel slope (β_c), associated with polarization measurements and the inhibition efficiency (IE %) at different inhibitor concentrations are listed in **Table 5.** It is obvious from **Fig. 4 and Table 5** that, according to I_{corr} and IE % values, the inhibitive properties of the studied surfactant inhibitor followed the order:

Inhib III > Inhib II > Inhib I

The surfactant inhibitors have the ability to inhibit both anodic and cathodic reactions because Tafel lines are shifted to more negative and more positive potentials with respect to the blank curve by increasing the concentration of the inhibitor. So they act as mixed type inhibitors [13]. This means that the inhibitors have significant effects on retarding both the cathodic reaction and inhibiting the anodic dissolution of carbon steel, [19].This behavior supports the adsorption of inhibitor onto metal surface and caused a barrier effect for mass and charge transfer for anodic and cathodic reactions,[33]. Lower corrosion current densities (I_{corr}) are observed with increasing the concentration of the nonionic surfactants inhibitors with respect to the blank without nonionic surfactants inhibitors, leading to decrease the corrosion rate. This effect can be attributed to the formation of a good protection film that isolate the metal surface from the aggressive environment. This behavior confirms a greater increase in the energy barrier of carbon steel dissolution process [7, 19-20].

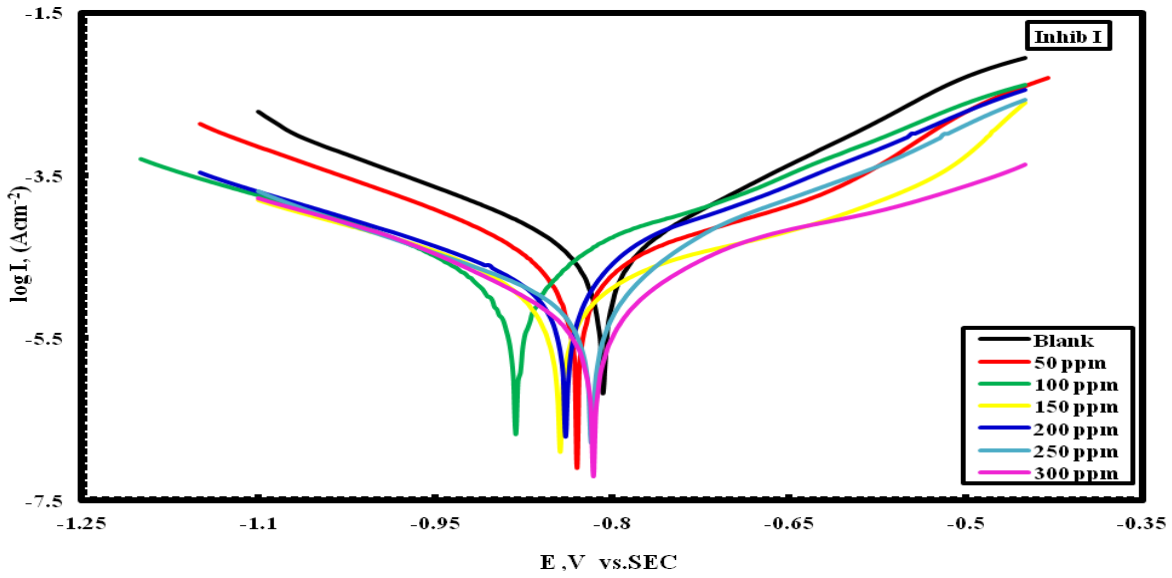

ISSN: 0975-8585

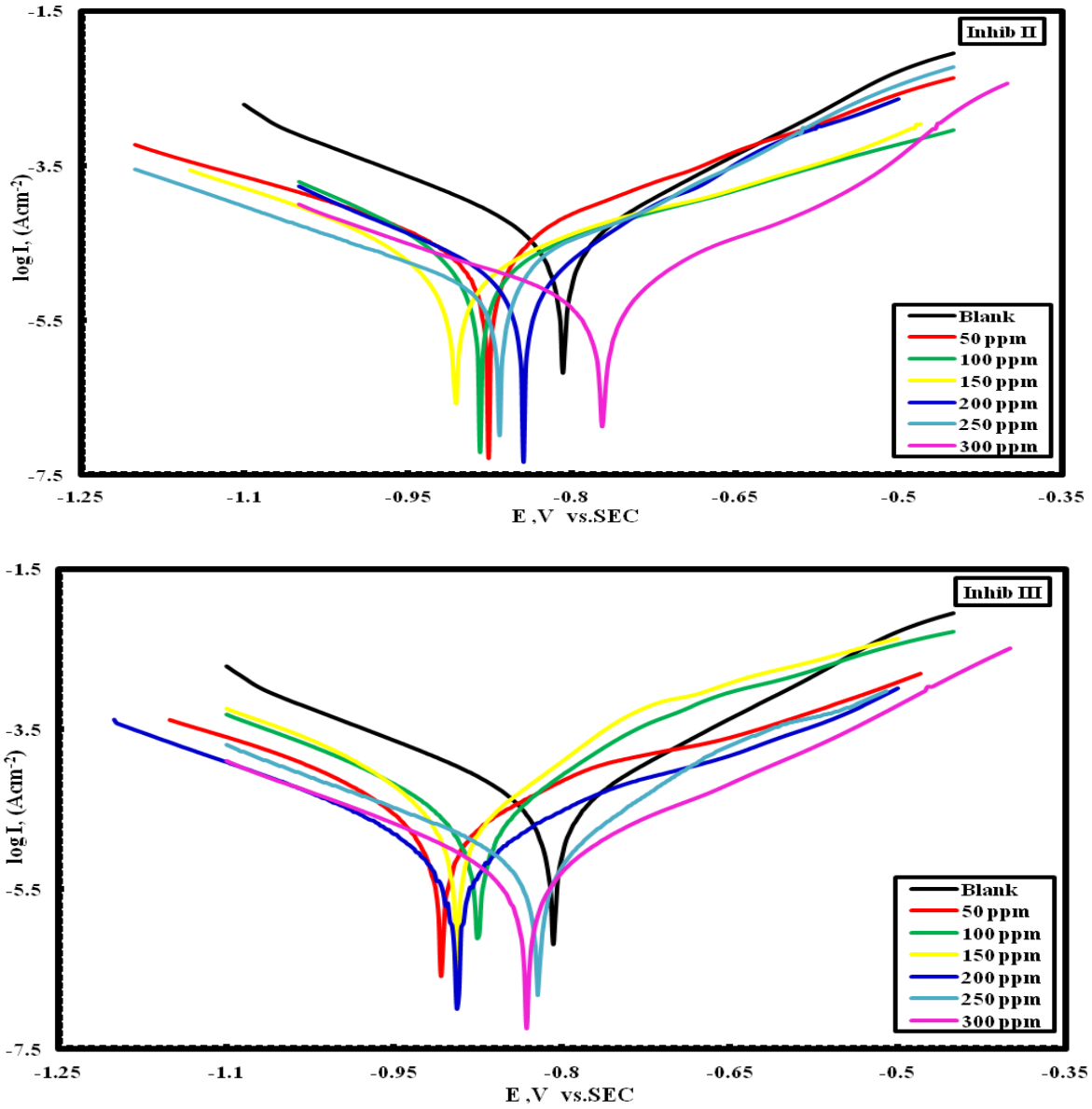

Figure 4: Potentiodynamic polarization curves for the carbon steel in oil wells' formation water saturated with CO_2 in absence and presence of various concentrations of investigated inhibitors (I, II and III) at 40 ºC

Obtain the results showed that ethoxylation of aniline (E_nA) with 15 , 25 and 35 degrees , then etherifying the ethoxylated amine with the Diels Alder product adduct (MOA) causes a decrease in the current density due to the newly existence of oxygen which increased as the degree of ethoxylated unite increased. Hence, the inhibitor effect is to reduce the current density to lower values (lower corrosion rate) as a result of increasing the function group which help in attaching the metal surface. The results can be attributed to the different in the molecular structure of both inhibitors.

Table 5: Electrochemical polarization parameters for the corrosion of carbon steel in the oil wells' formation water saturated with CO_2 in the absence and presence of various concentrations of investigated inhibitors at 40 ºC.

Inhibitor	Conc.	$-E_{corr.}$ (mV vs. SCE)	$I_{corr.}$ (µA/cm²)	R_p (K ohm.cm^2)	β_a (mVdec^{-1})	β_c (mVdec^{-1})	IE(%)
I	Blank	-833.4	39.9	1.24	311.6	-208.6	-----
	50	-833.4	25	1.54	151.9	-177.3	38.1
	100	-884.8	19.1	2.18	195.0	-183.3	52.0
	150	-847.7	13.9	3.37	318.7	-157.3	65.1
	200	-843.2	10.2	2.18	145.3	-156.6	74.6
	250	-821.0	7.7	3.51	104.8	-175.1	80.7

ISSN: 0975-8585

	300	-819.3	6.4	5.28	124.8	-166.5	84.0
II	50	-879.6	22.6	1.43	150.5	-177.4	43.4
	100	-887.1	17.2	2.08	258.7	-165.9	57.0
	150	-910.0	12.4	2.69	237.7	-182.2	69.0
	200	-824.0	8.9	3.36	116.1	-122.6	77.6
	250	-882.8	6.6	2.44	101.9	-126.0	83.5
	300	-774.7	4.7	5.63	116.2	-117.6	88.2
III	50	-910.8	20.1	1.78	134.6	-172.7	49.6
	100	-878.4	15.9	1.31	110.2	-133.2	60.2
	150	-897.2	13.2	1.16	95.6	-122.7	67.0
	200	-897.5	7.5	3.97	178.4	-179.6	81.1
	250	-825.0	5.5	3.99	113.8	-188.9	86.2
	300	-835.0	3.1	6.59	155.9	-178.2	92.2

The value of inhibition efficiency in **Table 5** is increased with increasing the inhibitor concentration from 50 ppm to 300 ppm while the maximum value of (EI %) is obtained for Inhibitor (Inhib III). [20, 33] It is clear that the corrosion current densities (i_{corr}) decrease with increasing inhibitor concentration. The effect was maximal for the concentration 300ppm, which is the optimum concentration of inhibitor required to achieve the efficiency (87%) This could be explained on the basis of inhibitor adsorption on the metal surface and the adsorption process enhances with increasing inhibitor concentration[20] .See **Table 5** the values of cathodic Tafel slope (B_c) and anodic Tafel slope (B_a) of surfactants are found to change with inhibitor concentration indicating that the inhibitors controlled both the two reactions, [33 and 34]. In other words, the inhibitors decrease the surface area for corrosion without affecting the mechanism of corrosion and only cause inactivation of a part of the surface with respect to the corrosive medium See **Table 5**. Indeed, accurate evaluation of Tafel slopes by Tafel extrapolation is often impossible, simply because an experimental polarization curve does not exhibit linear Tafel regions [19, 35].

3.4. Electrochemical Impedance Spectroscopy Measurements (EIS).

Fig. 5, shows the Nyquist plots of carbon steel immersed in oil wells formation water saturated with CO_2 in the absence and presence of various concentrations of the nonionic surfactants as corrosion inhibitors.

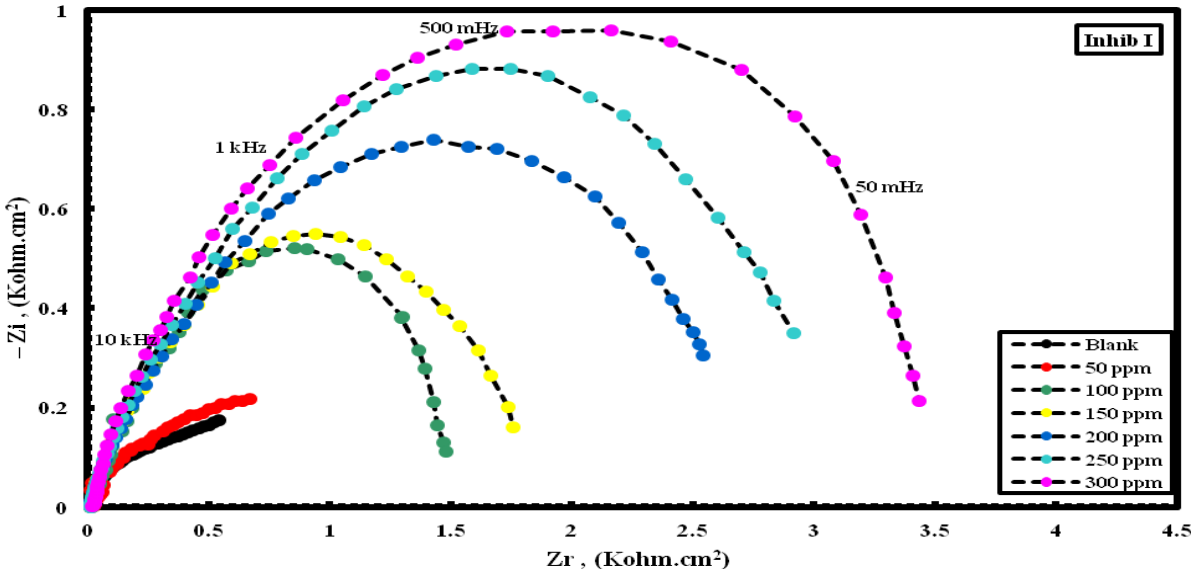

ISSN: 0975-8585

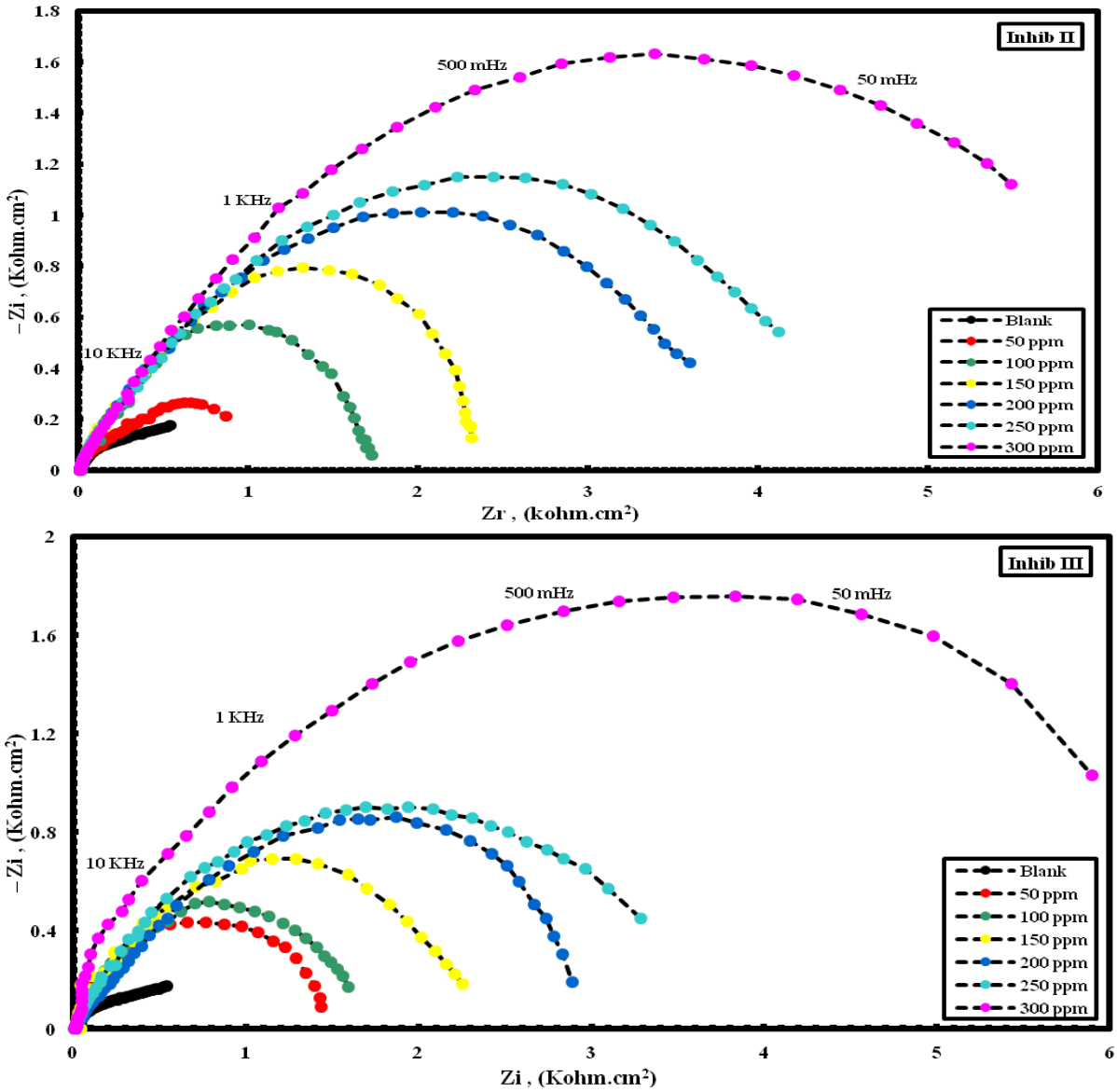

Figure 5: Nyquist plots for carbon steel in oil wells' formation water saturated with CO_2 in the absence and presence of different concentrations of investigated inhibitors at 40 ºC.

Table 6: Data obtained from electrochemical impedance spectroscopy (EIS) measurements of carbon steel in oil wells' formation water saturated with CO_2 in the absence and presence of various concentrations of investigated inhibitors at 40 ºC.

Inhibitor	Conc.	Rs $\Omega.cm^2$	n_1	R_f $K\Omega.cm^2$	C_f μFcm^{-2}	n_2	Rt $\Omega.cm^2$	C_{dl} μFcm^{-2}	IE %
I	Blank	6.5	0.88	-------	------	0.94	0.75	139.0	------
	50	13.1	0.90	0.036	46.7	0.81	1.24	52.4	39.5
	100	15.4	0.86	0.044	40.2	0.86	1.60	44.5	53.2
	150	20.2	0.77	0.047	35.3	0.79	2.19	33.3	65.8
	200	23.4	0.81	0.051	28.2	0.68	3.07	31.5	75.6
	250	26.5	0.79	0.057	26.4	0.80	3.98	29.1	81.2
	300	28.3	300	0.059	25.1	0.83	5.03	28.7	85.1
II	50	16.7	0.69	0.046	47.2	0.90	1.35	50.3	44.6
	100	18.1	0.91	0.048	41.6	0.78	1.82	42.6	58.7
	150	2o.3	0.87	0.053	36.3	0.75	2.51	32.8	70.2
	200	23.8	0.83	0.064	29.1	0.66	3.47	30.9	78.4

ISSN: 0975-8585

	250	27.2	0.77	0.068	27.5	0.85	5.20	28.7	85.6
	300	30.5	300	0.069	26.2	0.72	7.14	27.4	89.5
III	50	19.0	0.91	0.048	49.2	0.89	1.48	48.3	50.6
	100	22.3	0.78	0.052	46.5	0.85	1.98	31.8	62.3
	150	25.4	0.83	0. 056	38.5	0.76	2.41	29.7	68.9
	200	28.5	0.82	0.067	30.4.4	0.82	4.28	27.5	82.5
	250	29.2	069	0.069	28.9	0.68	6.04	26.8	87.6
	300	32.1	0.75	0.071	27.1	0.74	8.15	25.4	90.8

Curves have been obtained after 3h of immersion in the formation water saturated with CO_2. It has been reported that the Nyquist plots are generally associated with the charge transfer at the electrode/electrolyte interface [36]. EIS data are shown in **Table 6** and the suitable fitted by EIS analyzer equivalent circuit is program and shown in **Fig.5**.

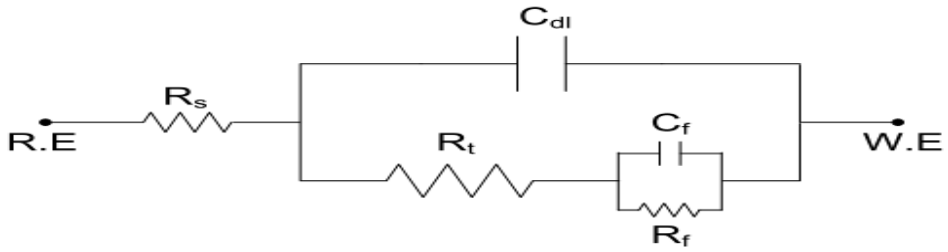

Figure 5: Equivalent circuit used to fitting impedance data of carbon steel in formation water at 30°C under CO_2 environment.

Where R_s is solution resistance, R_f is the film resistance, C_f is film capacitance, C_{dl} is the electrochemical double layer capacitance and finally R_t is the charge transfer resistance .The inhibition efficiency is calculated by charge transfer resistance obtained from Nyquist plots, according to the Eq. (15).

$$IE\ \% = 1 - \frac{R_{t\ Uninhib}}{R_{t\ Inhib}} \qquad (15)$$

$R_{t\ uninhibited\ and}$ $R_{t\ inhibited}$ without and with inhibitor, respectively. Various electrochemical parameters derived from Nyquist plots and IE% values were calculated and listed in **Table5** and listed in **Table 6**. The impedance data indicate that, the values of both IE % inhibition efficiency and R_t an increase in charge transfer resistance are found to increase by increasing the inhibitor concentration, while the values of C_{dl} are found to decrease. This behavior can be attributed to a decrease in dielectric constant and / or an increase in the thickness of the electrical double layer, suggests that the inhibitor molecules act by adsorption mechanism at carbon steel / formation water interface (9, 13, 33 and 37). The higher the R_t value is, the greater the resistive behavior of the steel, implying a more effective inhibitor. The increase in charge transfer resistance R_t for the inhibited system can be explained by an increase of the resistive behavior of steel owing to the formation of the adsorbed inhibitor molecules on steel surface. Results of EIS data show that IE % increases by increasing the inhibitor concentration reaching a maximum value at 300 ppm concentration. The order is in the following direction:

Inhibitor I < Inhibitor II < Inhibitor III

This order is in a good agreement with the data obtained from polarization techniques.

Surface Analysis:-

Scanning Electron Microscopy (SEM).

Fig. 7 (a) shows a characteristic inclusion observed on the polished carbon steel surface, which is probably an oxide inclusion (38). Hence, a comparison can be drawn with the morphology after exposure to the corrosive media. **Fig.7(b)** shows SEM image of the surface of carbon steel specimen after immersion in the oil wells formation water saturated with CO_2 for 30 days, while **Fig. 7 (c)** shows SEM image of another carbon steel specimen after immersion in the oil wells formation water saturated with CO_2 for the same time interval in presence of 300 ppm of the best inhibitor (Inhib III).

ISSN: 0975-8585

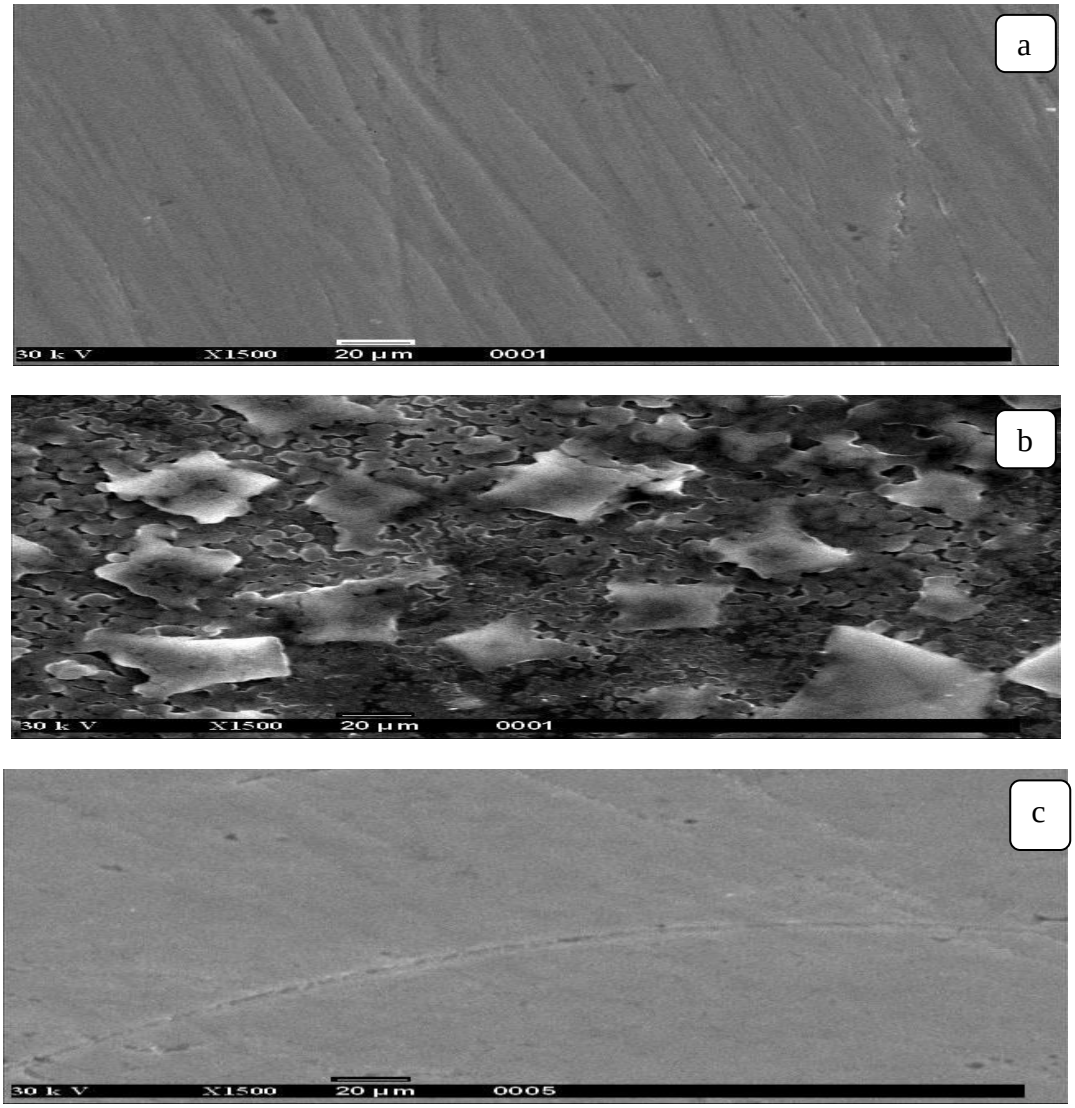

Figure 7: SEM images for the carbon steel surface: (a) polished sample, (b) after immersion in the oil wells formation water under sour conditions) and (c) after immersion in the oil wells formation water at 40 ^{o}C saturated with CO_2 environment in the in presence of 300 ppm of the best inhibitor (Inhib III).

The scanning electron micrographs reveal that, shows the surface is strongly damaged and observed as high surface roughness, owing to corrosion in the absence of the inhibitor, but in presence of the inhibitor, there is a much less damage on the surface. This may be attributed to the formation of a good protective film on the carbon steel surface. Hence, the inhibitor (Inhib III) provides good protection for the carbon steel surface against corrosion in the oil wells' formation water saturated with CO_2. The protective film formed on the carbon steel surface in presence of 300 ppm of inhibitor (Inhib III) appears to be very smooth and to cover the whole surface. This confirms the obtained high inhibition efficiency of inhibitor (Inhib III) from electrochemical measurements at 300 ppm concentration.

Energy Dispersive Analysis of X-Rays (EDX).

The EDX spectrum in **Fig. 8 (a)** shows the characteristics peaks of some of the elements constituting the polished carbon steel surface .The spectrum of the polished carbon steel surface after the immersion in the formation water saturated with CO_2 in absence and presence of 300 ppm of the best inhibitor (Inhib III) for 30 days, are shown in **Fig. 8 (b)** and (c) respectively. The spectra of **Fig. 8 (c)** show that the Fe peak is decreased considerably relative to the samples in **Fig. 8 (a) and (b).** This decreasing of the Fe band indicates that the strongly adherent protective film of inhibitor (Inhib III) is formed on the polished carbon steel surface, which leading to a high degree of inhibition efficiency [38].

ISSN: 0975-8585

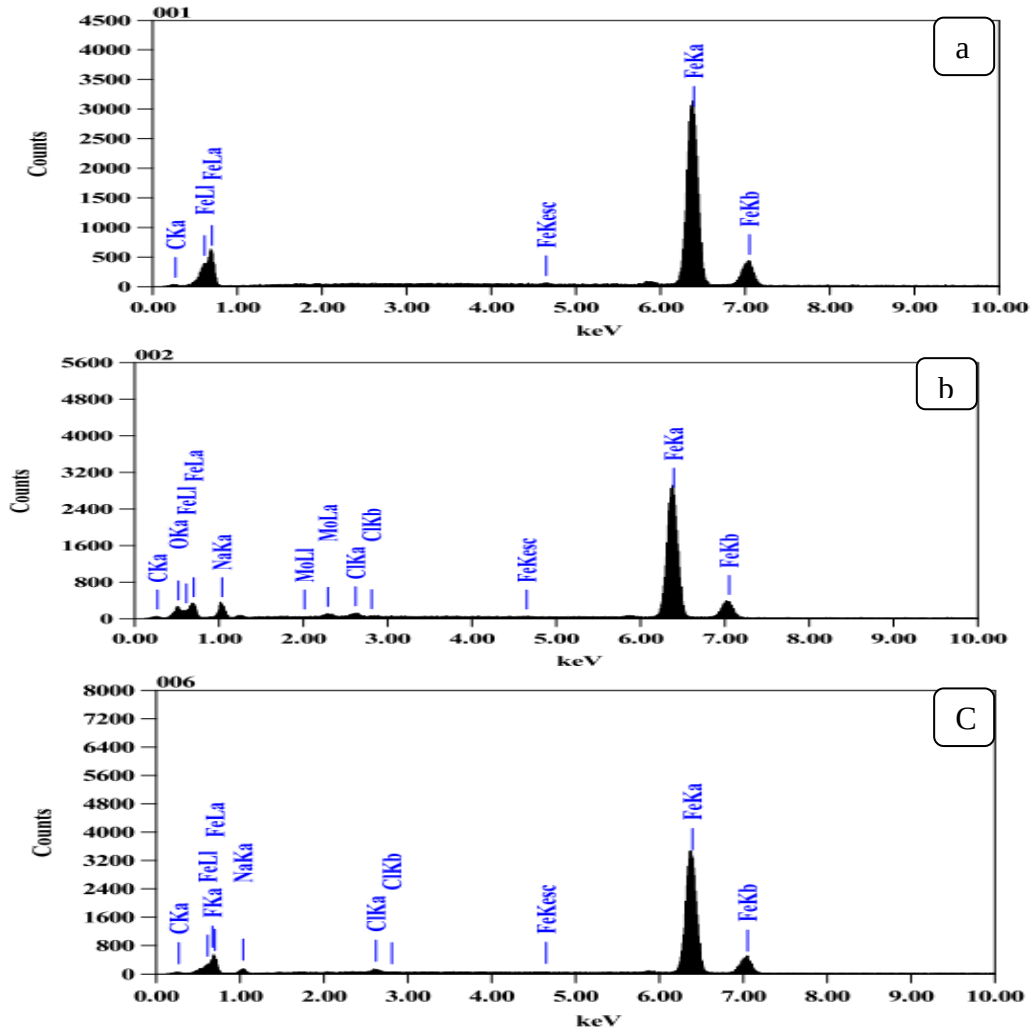

Figure 8: EDX of the carbon steel surface: (a) polished sample, (b) after immersion in the formation water and (c) after immersion in the formation water at 40 ºC saturated with CO_2 environment in the in presence of 300 ppm of the best Inhibitor (Inhib III).

The appearances of oxygen signal in **Fig. 9 (b)** is due to the carbon steel surface exposed to the formation water saturated with CO_2 in the absence of the inhibitor (Inhib III).Therefore, the EDX and SEM examinations of the carbon steel surface support the results obtained from the chemical and electrochemical methods that the synthesized surfactants inhibitors are a good inhibitor for the carbon steel in the oil wells formation water saturated with CO_2.

Quantum chemical study:

Computational study

Table 7 shows the calculated quantum chemical parameters for inhibitor I) which included, the energy of the highest occupied molecular orbital (E_{HOMO}), the energy of the lowest unoccupied molecular orbital (E_{LUMO}), the energy gap (ΔE), the dipole moment (μ) and logP.

Table 7 Quantum Chemical Parameters of the Investigated Inhibitors

Inhibitor	E_{HOMO} (eV)	E_{LUMO} (eV)	ΔE (eV)	μ (debye)	LogP	Polarizability (Å3)	Hydration energy, E_{hydr}, (k cal mol^{-1})	Surface area, A, (nm^2)	Total energy, E_T, (eV)
I	-6.67	0.283	6.953	2.74	4.50	116.23	-30.65	2059.16	-347994

ISSN: 0975-8585

According to the frontier molecular orbital theory, chemical reactivity can be considered in terms of interaction between the E_{HOMO} and the E_{LUMO}. E_{HOMO} indicates the tendency of a molecule to donate electron while E_{LUMO} indicates the tendency of a molecule to accept a lone pair of electron **[39]**.Therefore, higher value of E_{HOMO} and lower value of E_{LUMO} signify better inhibition efficiency. Careful examination of the experimental results reveals that based on increasing values of E_{HOMO} and on decreasing value of E_{LUMO}. This trend is consistent with results obtained from experiments.

The ΔE of a molecule is defined as the difference between the E_{LUMO} and the E_{HOMO} (i.e $\Delta E = E_{LUMO} - E_{HOMO}$). The ΔE of a molecule is a measure of the hardness or softness of a molecule **[40]**.Hard molecules are characterized by larger values of ΔE and vice versa. However, hard molecules are less reactive than soft molecules because the larger the gap between the last occupied orbital and the first virtual orbital, the more it is difficult for intermolecular electron transfer to proceeds. From the calculated values of the ΔE, the trend for the variation of the inhibition efficiency of the studied inhibitor with decreasing value of ΔE, is similar to that deduced from experimental data.

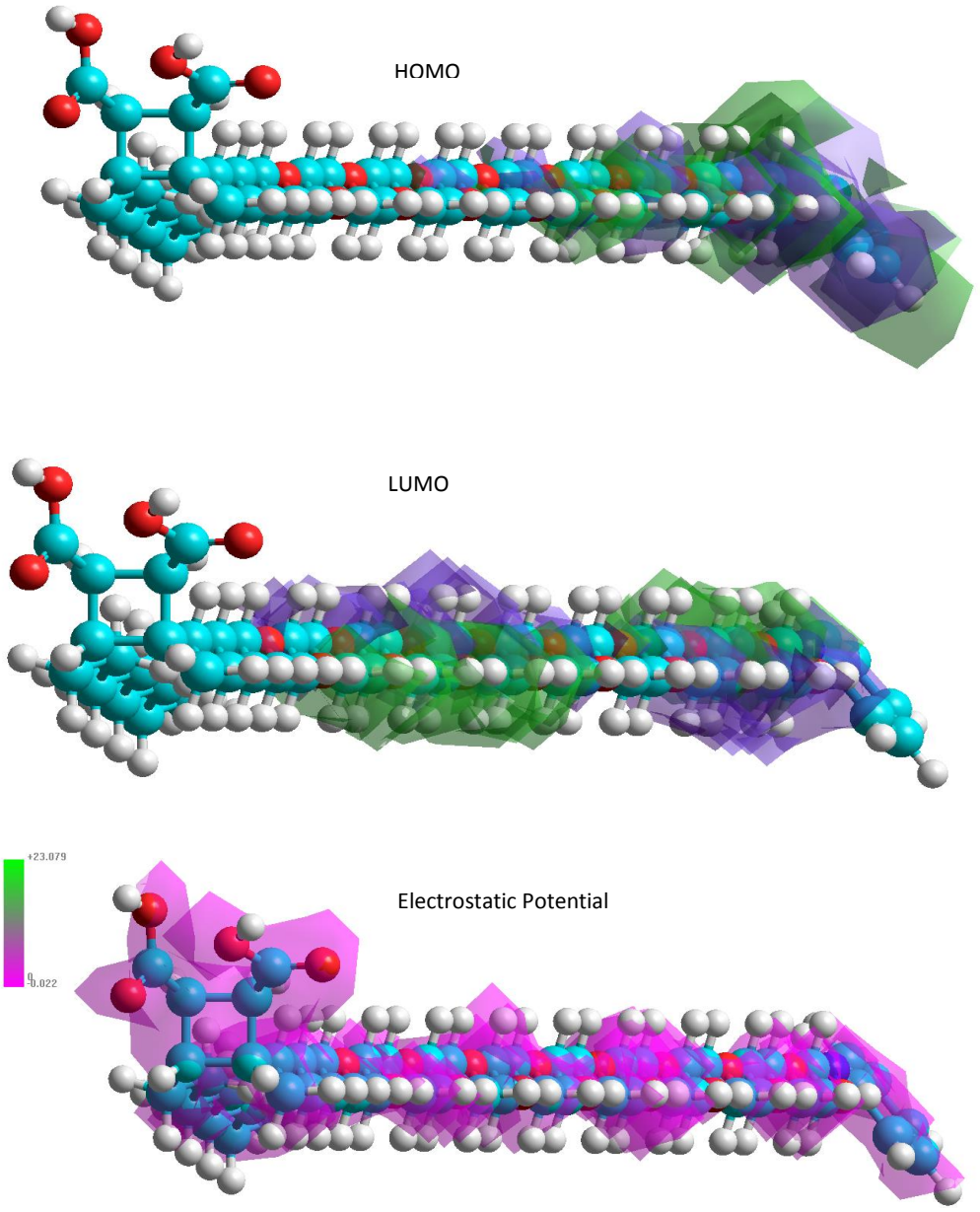

Figure 9: the frontier Molecular orbit density distribution for the investigated inhibitor.

μ is the measure of the polarity in a bond and is related to the distribution of electron in a molecule [41]. Although, there are some inconsistencies on the use of μ as a predictor for the direction of a corrosion inhibition reaction, it is generally agreed that the adsorption of polar compounds possessing high dipole moments on the metal surface should lead to better inhibition. Comparison of the results obtained from quantum chemical calculations with orbital experimental inhibition efficiencies indicated that the inhibition efficiencies of the inhibitors increase with decreasing value of μ. Also, it was found that the higher the value of logP, the more hydrophobic is the molecule hence water solubility is expected to decrease with increasing value of logP. From the point of view of corrosion inhibition process, the processes of inhibition that are affected by hydrophobicity are not well established. However, it is most probably that hydrophobicity can be used to predict the mechanism of formation of the oxide/hydroxide layer on the metal surface (which reduces the corrosion process drastically) [42]. From the results obtained, the inhibition efficiency of the studied inhibitors is found to increase with increasing value of logP. This trend supports experimental results. **Fig. 9** shows the (HOMO, LUMO) molecular orbitals of inhibitor I or a representation sample in addition to its electrostatic potential

Corrosion inhibition mechanism by surfactant molecule

The transition of metal/solution interface from a state of active dissolution to the passive state is of great interest [43]. Adsorption of the surfactant molecules occurs because the interaction energy between the surfactant molecules and the metal surface is higher than that between water molecules and the metal surface. So the inhibition effect by surfactants is attributed to the adsorption of the surfactant molecule via their functional groups onto the metal surface. The adsorption rate is usually rapid and hence the reactive metal is shielded from the aggressive environment. Corrosion inhibition depends on the adsorption ability of the surfactant molecules on the corroding surface, which is directly related to the capacity of the surfactant to aggregate to form clusters (micelles). The critical micelle concentration, CMC, is a key factor in determining the effectiveness of a corrosion inhibitor. Below CMC as the surfactant concentration increases, the molecules tend to aggregate at the interface, and this interfacial aggregation reduces the surface tension. Above CMC the metal surface is covered with a monolayer of surfactant molecules and the additional molecules combine to form micelles or multiple layers. This showed in **Fig. 3,** consequently, does not alter the surface tension and the corrosion rate [44].

CONCLUSIONS

1. All the investigated nonionic surfactants are effective inhibitors for corrosion of carbon steel in oil wells' Formation water saturated with CO_2.
2. The inhibition efficiency percentage of the surfactants increases by increasing the ethylene oxide units of inhibitor molecules.
3. The potentiodynamic polarization curves indicated that, the inhibitor molecules inhibit both anodic metal dissolution and also cathodic oxygen reduction, so that the undertaken surfactants classified as mixed type inhibitors.
4. A good correlation was observed between the EIS data and the results of polarization measurements.
5. The critical micelle concentration considers a key factor in determining the effectiveness of surfactants as corrosion inhibitors due to large reduction of surface tension at CMC.
6. The inhibition mechanism is attributed to the strong adsorption ability of the selected surfactants on carbon steel surface, forming a good protective layer, which isolates the surface from the aggressive environment.
7. The protection efficiency increases with increasing the inhibitor concentration.
8. The formation of a good protective film on carbon steel surface is confirmed using SEM and EDX techniques.

ACKNOWLEDGMENTS

I would like to thank all the staff members and all my friends in **EPRI** and **Egas** Company for their help and support. I would like to express my thanks and gratitude to **Dr. Eman Khames** for helping me in quantum chemistry.

ISSN: 0975-8585

REFERENCES

[1] Al-Sabagh, A.M.; Migahed, M.A. and Awad, H. S., Reactivity of polyester aliphatic amine surfactants as corrosion inhibitors for carbon steel in formation water, Corrosion Science 48 (2006) 813–828.

[2] Migahed, M.A.; Farag, A.A.; Elsaed, S.M.; Kamal, R .; Mostfa, M . and Abd El-Bary, H., Effectiveness of some diquaternary ammonium surfactants as corrosion inhibitors for carbon steel in 0.5 M HCl solution Materials Chemistry and Physics 125 (2011) 125–135

[3] Ortega-Toledo, D.M.; Gonzalez-Rodriguez, J.G.; Casales, M.; Neri-Florez, M.A. and Martinez-Villafañe, A., The CO_2 corrosion inhibition of a high strength pipeline steel by hydroxyethyl imidazoline, Materials Chemistry and Physics, 122 (2010) 485-490.

[4] Migahed, M.A.; Aly, R.O. and Al-Sabagh, A.M., Impact of gamma-ray-pre-irradiation on the efficiency of corrosion inhibition of some novel polymeric surfactants, Corrosion Science, 46 (2004) 2503–2516.

[5] Migahed, M.A.; Azzam, E.M.S. and Al-Sabagh, A.M.,Corrosion inhibition of mild steel in 1 M sulfuric acid solution using anionic surfactant, Materials Chemistry and Physics, 85: 2 (2004) 273–279.

[6] Farag, A. A. and Noor El-Din, M.R., The adsorption and corrosion inhibition of some nonionic surfactants on APIX65 steel surface in hydrochloric acid, Corrosion Science 64 (2012) 174–183.

[7] Migahed, M.A.; Abd-El-Raouf, M.; Al-Sabagh, A. M. and Abd-El-Bary, H.M., Effectiveness of some nonionic surfactants as corrosion inhibitors for carbon steel pipelines in oil fields,Electrochimica Acta,50:24(2005)4683-4689.

[8] Hegazy, M.A.; El-Tabei, A.S.; Bedair, A.H. and Sadeq, M.A., An investigation of three novel nonionic surfactants as corrosion inhibitor for carbon steel in 0.5 M H_2SO_4, Corrosion Science, 54 (2012) 219–230.

[9] El-Sabee, M. Z.; Morsi, R. E. and Al-Sabagh, A.M., Surface active properties of chitosan and its derivatives, Colloids and Surfaces B: Biointerfaces, 74 (2009) 1–16.

[10] Osman, M. M.; El-Ghazawy, R.A. and Al-Sabagh, A.M., Corrosion inhibitor of some surfactants derived from maleic-oleic acid adduct on mild steel in 1 M H_2SO_4, Materials Chemistry and Physics, 80 (2003) 55–62.

[11] Migahed, M.A.; Mohamed, H.M. and Al-Sabagh, A.M., Corrosion inhibition of H-11 type carbon steel in 1 M hydrochloric acid solution by N-propyl amino lauryl amide and its ethoxylated derivatives, Materials Chemistry and Physics, 80 (2003) 169–175.

[12] Negm, N.A.; Al Sabagh, A.M.; et al. Effectiveness of some diquaternary ammonium surfactants as corrosion inhibitors for carbon steel in 0.5 M HCl solution, Corrosion Science, 52 (2010) 2122-2132.

[13] Migahed, M.A.; Hegazy, M.A. and Al-Sabagh, A.M., Synergistic inhibition effect between Cu^{2+} and cationic gemini surfactant on the corrosion of downhole tubing steel during secondary oil recovery of old wells, Corrosion Science 61 (2012) 10-18.

[14] KERMANI. M. B. and SMITH. L. M. (eds.): 'CO_2 corrosion control in oil and gas production - design considerations', EFC Publication No. 23; 1997, London, The Institute of Materials.

[15] Bockris, J.O.M., Drazic, D., & Despic, A.R. (1961). The electrode kinetics of the deposition and dissolution of iron. *Electrochimica Acta*, 4, 325.

[16] Al-Sabagh, A. M.; Abdul-Raouf, M. E. and Abdel-Raheem, R., Reactivity of polyester aliphatic amine surfactants as corrosion inhibitors for carbon steel in formation water (deep well water), Colloids and Surfaces A: Physicochemical and Engineering Aspects, 251 (2004) 167-174.

[17] Negm,N.A. A.M. Al Sabagh, M.A. Migahed, H.M. Abdel Bary, H.M. El Din Effectiveness of some diquaternary ammonium surfactants as corrosion inhibitors for carbon steel in 0.5 M HCl solution CorrosionScience46(2004)2503–2516

[18] Marco Ormellese, Luciano Lazzari, Sara Goidanich, Gabriele Fumagalli, Andrea Brenna A study of organic substances as inhibitors for chloride-induced corrosion in concrete Corrosion Science 51 (2009) 2959–2968.

[19] Negm.N.A, Ghuiba. F.M, Tawfik. S.M, Novel isoxazolium cationic Schiff base compounds as corrosion inhibitors for carbon steel in hydrochloric acid Corrosion Science 53 (2011) 3566–3575.

[20] Zhang. G.A, Cheng. Y.F, Electrochemical characterization and computational fluid dynamics simulation of flow accelerated corrosion of X65 steel in a CO_2 saturated oil field formation water, Corrosion Science 52 (2010) 2716–2724

[21] Gao. M, Pang. X, Gao. K, The growth mechanism of CO_2 corrosion product films Corr. Sci. 53 (2011) 557–568

[22] Behr. A.; Fiene. M.; Naendrup. F.and Schürmann K., Eur. J. Lipid Sci. Technol., 342 (2000)

[23] Oppolzer W., Intermolecular Diels-Alder Reactions, in: ComprehensiveOrganic Synthesis,Vol. 5, Eds. Trost, B. M., and I.Fleming, Pergamon Press 1991, p. 315.

[24] Miller CA, Qutubuddin , Eike HF, Parfitt CD (E ds), Interfacial Phenomena in polar Media, 'Surfact ant Science Series', Vol. 21, (Marcel Dekker, Inc., New York 1 987), 166.

[25] Rosen MJ, in 'Surfactants and Interfacial Phen omena', (Wiley, New York, 1978), pp. 1–301.

[26] Atta. A M.; Dyab A.K. F. and Al-Lohedan H. A., JSurfactDeterg, 16, 343 (2013)
[27] Bentiss. F.; Lagrenee. M. and Traisnel.M.,Corrosion 56 (2000) 733.
[28] Omanovic. S. and Roscoe. S.G., Corrosion 56 (2000) 684.
[29] Hluchan. V.; Wheeler. B.L.and Hackerman. N,Werk, Korro. 39 (1988) 512.
[30] Amin. M.A.; Abd El Rehim. S.S.and Abdel-Fatah. H.T.M., Corros Sci. 51 (2009) 882.
[31] Migahed. M.A.; Abd-El-Raouf. M.; Al-Sabagh. A.M.and Abd-El-Bary. H.M., Electrochim. Acta 50 (2005) 4683.
[32] Bentiss .F.; Traisnel. M.; Chaibi. N.; Mernari. B.; Vezin.H.and Lagrenee. M.,Corros. Sci. 44 (2002) 227.
[33] Electrochemical and surface analysis studies on corrosion inhibition of Q235 steel by imidazoline derivative against CO_2 corrosion Wang. B, Du. M, Zhang. J, Gao. C.J, Corrosion Science 52 (2010) 2716–2724
[34] Zhihua Tao, Shengtao Zhang, Weihua Li, Baorong Hou, Corrosion inhibition of mild steel in acidic solution by some oxo-triazole derivatives Corrosion Science 51 (2009) 2588–2595
[35] William.Durnie,Roland.DeMarco,AlanJe.erson,Brian. Kinsella Harmonic analysis of carbon dioxide corrosion Corrosion Science 44(2002)1213–1221
[36] M. Hosseini, H. Tavakoli, T. Shahrabi, J. Appl. Electrochem. 38, 1629 (2008).
[37] Fuchs-Godec, Miomir. G, Pavlovic, Synergistic effect between non-ionic surfactant and halide ions in the forms of inorganic or organic salts for the corrosion inhibition of stainless-steel X4Cr13 in sulphuric acid, Corrosion Science 58 (2012) 192–201
[38] Migahed, M.A.; Abd-El-Raouf1, M.; Al-Sabagh, A.M. and Abd-El-Bary, H.M., Corrosion inhibition of carbon steel in acid chloride solution using ethoxylated fatty alkyl amine surfactants, Journal of Applied Electrochemistry, 36: 4 (2006) 395–402.
[39] Ebenso. E.E, Arslan .T, Kandemirli. F, Caner. N, I. Love, Int. J. Quant. Chem. 110 (2010) 1003.
[40] M. Sahin, G. Gece, F. Karci and S. Bilgic, J. Appl. Electrochem. 38 (2008) 809.
[41] Tanak.H, Yavuz.M., J. Molecular Modelling 16 (2010) 235.
[42] Eddy. N.O, Ebenso,E.E, J. Molecular Modeling 16 (2010) 1291.
[43] Malik MA , Hashim MA, F. Nabi , AL-Thabaiti SA , Khan Z, *Int. J. Electrochem. Sci*., 2011, 6, 1927 – 1948.
[44] Migahed MA, Abd-El-Raouf M, Al-Sabagh AM, Abd-El-Bary HM, *Electrochimica Acta,* 2005, 50, 4683– 4689